Journal of Nuclear Materials 406 (2010) 365–370

Contents lists available at ScienceDirect

Journal of Nuclear Materials

journal homepage: www.elsevier.com/locate/jnucmat

Archaeological analogs and the future of nuclear waste glass

Aurélie Verney-Carron [a,b,*], Stéphane Gin [a], Guy Libourel [b]

[a] Commissariat à l'Énergie Atomique (CEA), DEN, Laboratoire du Comportement à Long Terme, 30207 Bagnols-sur-Cèze, France
[b] Centre de Recherches Pétrographiques et Géochimiques (CRPG), BP 20, 54501 Vandoeuvre-lès-Nancy Cedex, France

ARTICLE INFO

Article history:
Received 2 July 2010
Accepted 14 September 2010

ABSTRACT

Nuclear energy produces long-lived radioactive waste. Glass containment matrices are used to stabilize such waste and to prevent radionuclide dispersion. Over the past few decades, phenomenological models have been developed to predict the long-term behavior of these materials in anticipation of disposal in a deep geological formation. But considering the geological time scales necessary for radioactive decay validating these models is a challenge. Here we show how the validation of the predictive capacity of a mechanistic model applied to archaeological glass alteration bridges the gap between the short-term laboratory data and the long-term evolution of natural system in complex environment. This model applied to nuclear glass provides reliable uncertainties on long-term alteration rates and demonstrates that present models used in the safety calculations are conservative.

1. Introduction

Spent nuclear fuel management is a major societal issue, especially in countries that wish to pursue the development of nuclear power. Many countries carry out, for civil and/or military purpose, separation of reusable fissile materials (uranium and plutonium) and immobilization of the fission products and minor actinides, notably by vitrification. At the present time nearly 15,000 metric tons of glass have been produced, mainly in France, Belgium, United States, Great Britain, and Russia. These glass packages contain some 2.5×10^{20} Bq. As an illustration, this activity globally represents the HLW produced by twenty-three 1 GWe reactors operating for 40 years.

After five decades of debate on the management of long-lived high-level waste (spent nuclear fuel or nuclear glass packages), a broad consensus has taken form in favor of long-lived high-level waste storage in a deep geological repository. Except the Waste Isolation Pilot Plant in the New Mexico desert (devoted to defense related transuranic waste), no other geological repository site is yet in operation. However, most countries have initiated a site selection process. Studies to demonstrate the long-term safety of this option are based on phenomenological modeling because of the very long time scales (10^4–10^5 years for a drastic reduction of the radioactivity) and also the nonlinear coupling of the phenomena involved [1].

One One of the requirements to opening a repository is to demonstrate to the authorities and the public that reliable simulations can be carried out over such durations. Concerning the prediction of HLW glass durability, the use of natural and archaeological analogs becomes indispensable to validate these simulations because some of these materials have been altered for very long times moreover in natural (complex) environments [2–4].

For the countries that reprocess spent fuel, the containment borosilicate glass constitutes the primary barrier against radionuclide release (Fig. 1). But during the cooling of the package, the glass becomes cracked as mechanical stresses are released [5]. Most of the cracks in the glass package are radial and concentric (Fig. 1). Whatever their subsequent disposition, nuclear glasses will be subjected to self-irradiation, which is capable of modifying their microstructure and their mechanical properties; even over the long-term, however, these effects are considered negligible or even beneficial (hardness reduction and increased resistance to cracking) (e.g. [6,7]). Under geological repository conditions (in a deep clay formation in France), and despite the low permeability of the rock and the presence of additional containment barriers (a steel overpack and in some designs an engineered barrier), aqueous alteration will be inevitable. The radionuclides confined in the glass can then dissolve and, for the most mobile among them, migrate into the aquifer. Therefore, the safety models have to consider the rate of radionuclide release, caused by aqueous alteration of the glass, their migration through the backfilling materials and the geological barrier, and their transfer towards biosphere.

The radionuclide flux is estimated from the quantity of altered glass (QAG) over time as radionuclides are homogeneously distributed in the glass:

* Corresponding author. Present address: Laboratoire Inter-universitaire des Systémes Atmosphériques (LISA), 61 avenue du Général de Gaulle 94010 Créteil Cedex, France. Tel: +33 1 45 17 65 70; fax: +33 1 45 17 15 64.
E-mail address: aurelie.verney@lisa.u.-pec.fr (A. Verney-Carron).

0022-3115/$ - see front matter © 2010 Elsevier B.V. All rights reserved.
doi:10.1016/j.jnucmat.2010.09.028

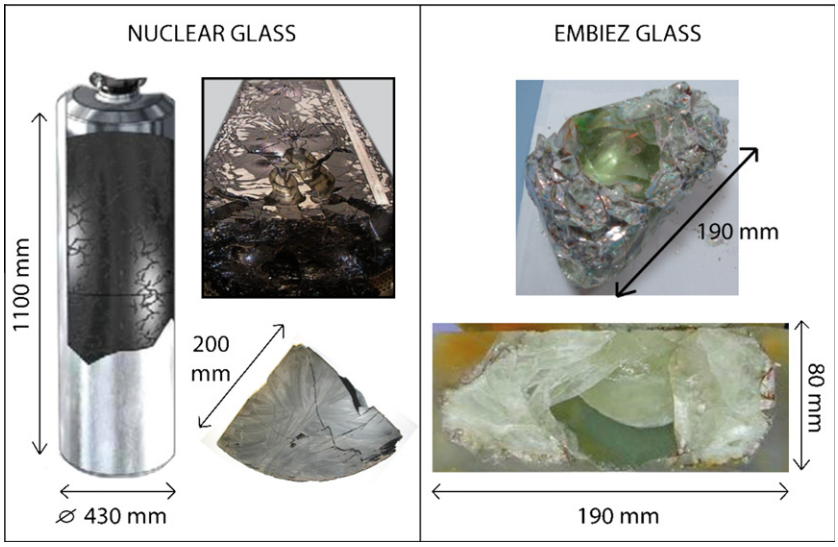

Fig. 1. Fractured nuclear and archaeological (Embiez) glass blocks. (a) Nuclear glass: diagram of a French R7T7-type glass package produced in the La Hague R7 and T7 facilities, longitudinal cross section and partial cross section of a block. The cracking factors are 5 (considering major cracks) and 40 (considering all cracks accessible to solution) (Gin et al.). (b) Archaeological glass: complete block and longitudinal cross section.

$$\mathrm{QAG} = \int \int_{t,S} r(t,S) \cdot dS \cdot dt \tag{1}$$

where r is the glass dissolution rate, t the time, and S is the reactive surface area.

To solve Eq. (1) is complex as alteration kinetics of glass and minerals are highly dependent on local chemical conditions [8], time [9], and surface location (external surfaces directly in contact with the surrounding environment or isolated internal cracks). Faced with these difficulties, the models used for safety analysis adopt a simplified and conservative approach by decoupling the rate and surface area terms [10]. But to strengthen the safety demonstration and justify these simplifications, Eq. (1) must be solved in reference cases by using geochemical codes [11].

In this paper, we present a geochemical model of archaeological glass alteration coupled with transport to simulate the long-term alteration (over 1800 years) of fractured glass blocks. By confronting the results of simulation with the observations (phenomenology and apparent kinetics) and therefore by demonstrating the predictive capability of this model, we can infer the implications for the long-term behavior of nuclear glass in a geological repository.

2. Materials and methods

2.1. Samples

Ancient Roman glass blocks, discovered in a shipwreck in the Mediterranean Sea near the French Embiez Island, were chosen because of well-known and stable alteration conditions.

They certainly had been fabricated in the eastern Mediterranean (Syro-Palestinian Coast or Egypt) near the sites where the raw materials were mined, and were destined for remelting in finishing workshops in the western Mediterranean [12]. They have been dated archaeologically to the second century AD [12] and were therefore leached for 1800 years in seawater at a constant temperature of 15 °C.

The blocks were fractured due to rapid cooling after melting, as nuclear glasses (Fig. 1). The archaeological glass blocks come from a glass slab that was melted in a large furnace and cooled in air. This elaboration technique is evidenced by the presence of some blocks with plane surfaces and some blocks with less melted glass (opaque) probably located at the bottom of the furnace [12]. The thermal stress release during the cooling caused its fracturing. Then the slab was crushed into blocks of a few kilograms on average (until 25 kg for the heaviest blocks) to be shipped to Europe, where they would have been annealed and manufactured [12].

The glass blocks were lying on the seafloor and were partially recovered by sand [12]. However, they were not included in a sand matrix.

Their composition was analyzed using a 4 kW Wavelength Dispersive X-ray Fluorescence (WDXRF) spectrometer (Pioneer S4, Bruker AXS) and is that of a typical Roman glass, i.e. a soda-lime silicate glass (approximately 70% SiO_2, 20% Na_2O, 5% CaO, 1.8% Al_2O_3 and 3.2% others) [13]. The low content in MgO (<0.4%) and in K_2O (<0.4%) corresponds to the use of evaporitic minerals (natron) as a melter [14]. Their composition is different from borosilicate nuclear glass, as the latter present a higher silica content around 45% SiO_2 for the French R7T7 glass [10]) and no boron. However, both are silicate glasses and the analogy of mechanisms and kinetics will be discussed.

The crack network and the alteration products were observed by SEM–EDS (Scanning Electron Microscopy–Energy Dispersive X-ray Spectroscopy) using a JEOL JSM-6330F with an accelerating voltage of 15 kV. Samples were embedded in epoxy resin, then polished using SiC paper (1200) and diamond suspensions (9–3–1 μm), and carbon-coated.

Characterization of the crack network was performed from two-dimensional trace maps. The length, the alteration thickness, and the orientation of 2000 cracks were measured. In order to determine three-dimensional geometric parameters, as the crack density or the fracture ratio, and the percentage of alteration, stereological relations were used following the relations from [15] and [16].

The fracture ratio (FR) corresponds to the ratio between the surface area developed by the cracks (S_{cracks}) and the geometrical surface area of the block (S_{geo}). The fracture ratio can be expressed as the surface of both walls of one crack considered as a disk (with a mean radius R_m) multiplied by the number of cracks:

$$FR = \frac{S_{cracks}}{S_{geo}} = \frac{2 \cdot \pi R_m^2 \cdot \rho \cdot V}{S_{geo}} \tag{2}$$

with ρ the crack density and V the volume of the glass block.

The alteration percentage is the ratio between V_{alt} the altered volume and V the volume of the glass block. V_{alt} is calculated as the altered volume of one crack multiplied by the number of cracks:

$$V_{alt} = \pi R_m^2 \cdot e_m \cdot \rho \cdot V \quad (3)$$

with e_m the average alteration thickness.

The alteration products were analyzed by Electron Probe Micro-Analysis (EPMA) using a Cameca SX-100 electron microprobe Henri Poincaré University (Nancy, France), which is equipped with five spectrometers and a wavelength–dispersive system (WDS). The accelerating voltage and current intensity were 15 keV and 8–10 nA, respectively. The mineralogy of the alteration products was determined by in situ X-ray diffraction using a photon microprobe developed at the Pierre Süe Laboratory (CEA/CNRS, France), which is built on a rotating anode X-ray generator. The beam delivered by a molybdenum (17.45 keV) anode is focused on a surface of 20 μm × 20 μm by a borosilicate capillary. Micro-XRD patterns were collected in transmission mode, so downstream thin sections (500 μm), by a 2D image plate detector and were obtained after circular integration using the FIT2D program developed at the European Synchrotron Radiation Facility (ESRF).

2.2. Modeling

A geochemical model was developed to simulate the alteration of the archaeological glass. The kinetic parameters were determined by experiments [17]. This model was coupled to diffusive transport in solution to simulate alteration in cracks using HYTEC code that is developed by the *École Nationale Supérieure des Mines de Paris* (ARMINES-CIG/ENSMP) [18].

3. Results

3.1. Phenomenology and kinetics of alteration

SEM observations showed that the cracks of Embiez glass were filled by alteration products and presented two alteration morphologies (Fig. 2b and c [13]). The cracks directly in contact with the bulk seawater until a depth of 1 cm showed total alteration thicknesses of about 500 μm and were filled with magnesium smectites (XRD) (Fig. 2b) formed by dissolution of the glass network and precipitation of the least soluble elements (Si, Al) together with some elements from the seawater, especially Mg, almost absent from the glass, but at a high concentration in seawater ($[Mg^{2+}]$ = 1.28 g/kg). A thin amorphous hydrated glass layer about 1 μm thick containing no sodium is visible in some places at the interface between the pristine glass and the smectites. These alteration thicknesses are similar to the Iulia Felix glass fragments, whose pristine glass composition is very close to the Embiez glass blocks and which date from the same period (II century AD). The total alteration thicknesses of Iulia Felix samples vary from 200 to 1500 μm, whereas the gel layer thicknesses are between 10 and 100 μm [19]. However, the fragments were buried in carbonatic sand and subsequently cemented by calcite [19]. In the Embiez glass blocks, the internal cracks are connected to the peripheral cracks but they form a much denser network. Their alteration thicknesses are thinner, between 5 and 30 μm (Fig. 2c). They consist of an amorphous hydrated glass layer and a thin (1–5 μm) smectite layer at the center of the crack (Fig. 2c).

At the scale of the block, the fracture ratio is 86 ± 27. Although the cracks considerably increase the reactive surface (86 times) they ultimately have a relatively minor role in glass alteration [13]. Thanks to stereological analyses, after 1800 years, the overall altered glass volume was determined and is 12.2 ± 4.1%, of which 7.4 ± 1.7% is due to the external cracks and only 4.8 ± 1.2% to the internal cracks, although the latter are six times more numerous [13].

3.2. Modeling of the alteration

A kinetic model of archaeological glass alteration was developed to account for these findings. The details of the modeling are given in [17]. Briefly, three mechanisms were considered: (1) the interdiffusion of alkalis from the glass and hydrogen species from the solution that leads to the formation of a hydrated layer; (2) the dissolution of the hydrated layer up to the saturation of the solution with respect to silicon and (3) the precipitation secondary phases. The concentration in alkalis, especially in sodium, in solution evolves with the square root of time and is highly dependent on the glass surface area/solution volume ratio. Therefore, the kinetics of alkalis diffusion into solution was experimentally determined by following the Na concentrations in solution as a function of the temperature and pH and by deducing a diffusion coefficient D thanks to the second Fick's law. The results gave the following relation:

$$D = 0.678 \cdot [H^+]^{0.37} \cdot \exp(-93,600/RT) \quad (4)$$

with R the ideal gas constant and T the temperature.

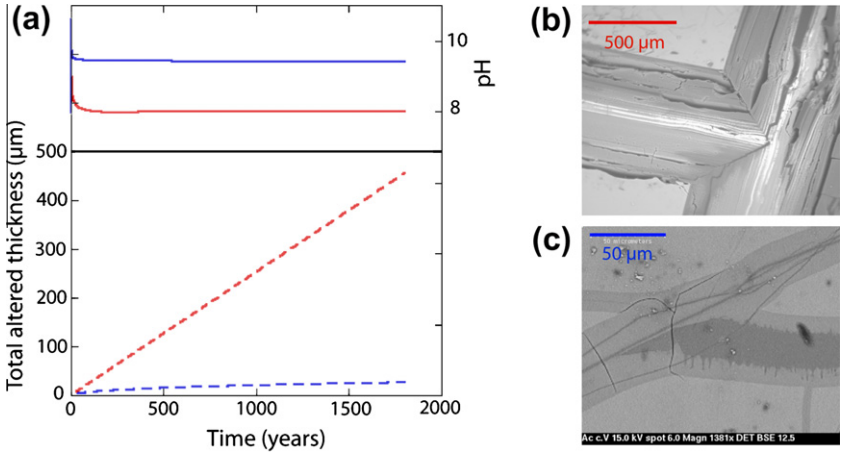

Fig. 2. Simulated solution pH and total alteration thickness versus alteration time for a crack with a 100 μm initial aperture at 1 cm from the external surface (in red) and from a crack with a 2 μm initial aperture (without sealing) at 5.6 cm from the block (in blue). The results are compared with SEM observations of alteration thicknesses for a crack in direct contact with the border of the block (red) and for internal cracks (blue).

The dissolution rate of the hydrated layer was measured in 'far from equilibrium' conditions in order to determine the initial rate r_0 as a function of pH and temperature and in 'close-to-equilibrium' conditions in order to parameter the affinity term that controls the dissolution rate drop. The dissolution rate r is given by:

$$r = r_0 \cdot (1 - [H_4SiO_4]/K_{SiO_2}) \quad (5)$$

with K_{SiO2} the equilibrium constant equal to the solubility product of cristobalite β.

The initial dissolution rate r_0 is equal to:

$$r_0 = 6.73 \times 10^9 \cdot [H^+]^{-0.32} \cdot \exp(-85,600/RT) \quad (6)$$

The values of the kinetic parameters are discussed below.

The formation of secondary phases is controlled by thermodynamic equilibrium. The choice of the phases allowed to precipitate is based on the experimental observations and on the glass blocks characterization.

In order to simulate the alteration of the cracks, the geometric system was defined as a crack in a glass whose tip is in contact with a continuously renewed medium of seawater at 15 °C. The tested parameter is the initial crack aperture. The transport in solution inside the crack is controlled by a diffusion coefficient in solution that is equal to the diffusion coefficient in free water ($\approx 10^{-9}$ m^2 s^{-1}).

Fig. 2a displays simulations over 1800 years of the alteration of two types of cracks: one with a 100 μm initial aperture at 1 cm from the external surface (in red[1]) and the other with a 2 μm initial aperture (without sealing) at 5.6 cm from the block (in blue). The first type of cracks is representative of large peripheral cracks and the second one corresponds to thinner and more isolated internal cracks. Fig. 2a represents the evolution of the pH and the total altered thickness with respect to the time. For the large crack, the pH reaches quickly the pH of seawater because the crack is large enough to allow a continuous renewal of the solution. In the thin internal crack, the pH rises to 9.4. The renewal of the solution by diffusion is too low to counterbalance the increase in pH caused by ion exchange between the alkalis of the glass and the hydrogen species in solution. The consequence on the altered thickness is significant. After 1800 years of alteration, the altered thickness is around 450 μm for the large crack and around 30 μm for the thin internal crack. The dependence on the alteration thickness to the initial aperture of the crack is consistent with experimental studies (e.g. [20]).

These results are in good agreement with the observations. The total thickness of cracks in the archaeological glass block ranges from 5 to 30 μm for the internal cracks and from 400 to 500 μm for the external cracks (Fig. 2, [17]). Coupled with diffusive transport of aqueous species and extrapolated over 1800 years, the model developed for Embiez glass highlights the significant effect of the initial crack aperture and of the location of the crack. Therefore, the model accurately and quantitatively simulates alteration kinetics in the cracks by coupling chemistry and diffusive transport (Fig. 2). The large cracks have been altered for 1800 years at the maximum rate r_0 because of continual water renewal, and the internal cracks with thinner alteration layers due to the leaching kinetics limited by water diffusion in the glass after rapid silica saturation in solution.

Both cracks shown here are considered to be representative of both populations of cracks in the block: the external cracks directly in contact with seawater (to a depth of about 1 cm in the block) and the internal thin cracks. The altered glass percentage was calculated over time (Fig. 3a) allowing for the reactive surface areas of the two types of cracks ($S_{ext} = 7 \times S_{geo}$ and $S_{int} = 79 \times S_{geo}$). The block was leached mainly via the external cracks and the contribution of the internal surfaces diminished continuously over time (Fig. 3a). If only the internal surfaces were leached, more than 650,000 years would be necessary for complete alteration of the Roman glass blocks, but external surfaces alteration would limit the lifetime to about 20,000 years.

[1] For interpretation of color in Figs. 1–3, the reader is referred to the web version of this article.

4. Discussion

4.1. Legitimacy of the transposition of the model to nuclear glass

The predictions of the archaeological glass model cannot be transposed directly to nuclear glass. The consistency between the simulations of the archaeological glass model whose kinetic parameters were determined thanks to short-term experiments and the long-term observations demonstrates that the alteration mechanisms considered in the model are long-term predominant mechanisms and validates the shift from short-term to long-term. It therefore improves the confidence in long-term predictions. The shift from one glass to another requires the demonstration of the mechanistic analogy between archaeological and nuclear glass [2,3].

The kinetic laws corresponding to the mechanisms observed for the archaeological glass model (interdiffusion and dissolution/precipitation) are largely inspired by work on minerals [8,21,22] and nuclear glasses [23].

The mechanism of interdiffusion that transforms the glass into a hydrated and dealkalinized layer is also observed on nuclear glasses [23–26]. The parameters of the diffusion kinetic law (pH-dependence coefficient and apparent activation energy) determined for the archaeological glass [17] are similar to those determined for nuclear glasses [23,27] and for obsidian [28,29]. Indeed the activation energies determined by [23,27,28] range between 80 and 90 kJ/mol, consistent with archaeological glass (94 kJ/mol) (Eq. (4)). The pH-dependent coefficient (relative to $[H^+]$) is 0.325 for nuclear glass [27] and 0.49 for obsidian [29], also similar to Roman glass (0.37, Eq. (4)). However, the diffusion coefficients for archaeological glass are four orders of magnitude higher than for borosilicate glass [17,27]. For example, at 25 °C and pH 8, the diffusion coefficients of alkalis are 3×10^{-20} m^2/s and 2×10^{-24} m^2/s for Roman glass and R7T7-type glass, respectively. Structural differences due to the composition of the glass can infer differences in the reorganization of the hydrated glass or gel layer and on its passivating role [30–32].

The dissolution of the hydrated glass that progresses until a kind of equilibrium is reached in solution follows a rate law comprising a pH- and temperature-dependent kinetic constant and a chemical affinity term, as in the case of nuclear glasses [23,33]. The activation energy of the archaeological glass initial dissolution at the pH of seawater was found to be 75.6 kJ/mol [17], which is comparable to R7T7 glass (71 kJ/mol, [34]) and to basaltic glass (72.4 kJ/mol, [35]) at neutral or slightly alkaline pH. Generally, the activation energy of silicate dissolution varies between 50 and 90 kJ/mol (e.g. review of [36]). The coefficient of pH dependency is also close to those determined for R7T7 (0.41 at 90 °C, [37]) and basaltic glasses (0.35 at 100 °C, [38]), as well as for other silicate minerals [39].

For comparison, at pH 8 and 25 °C, the initial dissolution rate r_0 is 0.0092 g/m^2/d for R7T7-type glass [33] and 0.0025 g/m^2/d for Roman glass (Eq. (6)). The difference of glass compositions affects also the nature of the phase controlling the rate drop [17]. The solubility product of the phase that controls the rate drop is close to the solubility product of the chalcedony for R7T7-type glass [40]. For Roman glass the solubility product of the silica phase is higher,

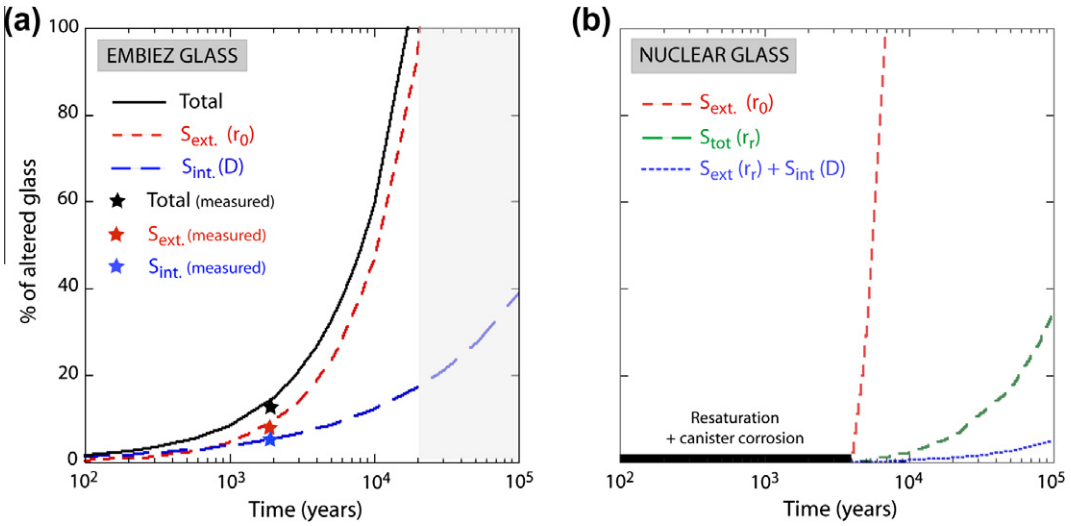

Fig. 3. Predicted percentage of alteration for Embiez (left) and nuclear (right) glass block. Several rate regimes (initial rate r_0, residual rate r_r and diffusion-controlled rate D) are tested for external (S_{ext}) and internal (S_{int}) surfaces. For Embiez glass the predicted and measured values are in agreement. But the lifetime is limited to 20,000 years because of unfavorable environmental conditions.

as it is close to the cristobalite β (Eq. (5)). The nature of secondary phases allowed to precipitate in the model is determined from short and long-term observations is similar for all types of glass, mainly clay minerals, especially smectites, carbonates, and zeolites [13,17,33,41].

In summary, the main mechanisms (interdiffusion, dissolution, precipitation) are common to all silicate glasses and only the kinetic and thermodynamic parameters are glass dependent. The analogy between basaltic glass and nuclear glass was also established based on field observations and phenomenological similarities concerning the alteration layers [41–46] and on experimental kinetics determination [35,41]. These results and this study strengthens the reasoning by analogy [2,3]. Considering the large discrepancies between field and laboratory-measured alteration rates (the first ones being smaller than the second ones) for basaltic glasses and minerals or rocks (e.g. [9]), it can be inferred that the results of glass alteration models for nuclear glass are conservative [47]. These differences can be caused by the progressive depletion of surface sites, the formation of leached layers, the secondary phase formation, the evolution of the solution... [9,47]. Concerning the glass alteration modeling, the current archaeological glass model is very similar to the GRAAL model recently developed to predict the R7T7-type glass dissolution alteration [33,40].

The Embiez archaeological glass was also specifically chosen to better understand the alteration in cracks, as nuclear glass blocks are fractured during their elaboration process. The contribution of the reactive surfaces developed by the fracturing remains a source of uncertainty in the nuclear glass model. The transposition of the Embiez glass model can be useful to assess the uncertainties on the present assumptions in the nuclear glass model and to refine the predictions.

4.2. Application to nuclear glass alteration

A similar calculation of the lifetime of a fractured nuclear glass package confined in a geological repository was performed by taking into account the requirements of safety assessments: simplicity, robustness, and conservatism.

The numerical application is indicated for the French R7T7-type glass, but can be transposed to other borosilicate glasses as the orders of magnitude of the parameters are comparable [48,49]. Different cases were considered. The temperature, caused by the heat from radioactive decay, is assessed to be around 50 °C after 4000 years, i.e. the time necessary for the contact with aqueous solution and the corrosion of the steel barriers (primary canister and overpack) [50].

The glass package presents external (S_{ext}) and internal (S_{int}) surfaces. The geometric surface area of a package is 1.7 m^2 [10] and considering the fracture ratio determined for R7T7-type glass, the external surface area is 8.5 m^2 and the internal surface area is 68 m^2 [10]. According to the different cases considered, several rate regimes (initial rate r_0, residual rate r_r and diffusion-controlled rate D) are tested. For R7T7-type nuclear glass, the initial rate r_0 is equal to 5.1 μm $year^{-1}$ and the residual rate r_r to 0.008 μm $year^{-1}$ [33]. The diffusion coefficient D of the mobile elements (i.e. alkalis and boron) for R7T7-type glass at 50 °C and neutral pH is 6.8×10^{-23} m^{-2} s^{-1} [27].

The most conservative approach assumes the glass is altered continuously at its maximum rate (e.g. [51] for the Belgium approach), which involves a rapidly renewed solution medium, as in the case of the Embiez glass. In this case a standard 400 kg glass package would release its radionuclides inventory into the near-field in less than 8000 years (red curve, Fig. 3b). In a waste repository, however, the very low permeability and isolation of the clay [50,52] constitutes a highly confined medium favoring low alteration rates. The second approach, adopted in France [10,50], Switzerland, and Japan, therefore assumes that the glass is altered at a residual rate that considers the effects of saturation in solution, the passivating role of the alteration layer and the slow precipitation of secondary crystalline phases. In this case, assuming a brief transient regime (during which the maximum rate is maintained), less than 40% of the glass block would be altered after 100,000 years and the package lifetime would be about 300,000 years (green curve, Fig. 3b). Finally, if the external surfaces of the glass block are altered under residual rate and the kinetics within the internal cracks are controlled by water diffusion in the glass after the sealing of the cracks (in accordance with what was observed, modeled and validated for the archaeological glass), the calculations show that the glass would be altered even more slowly: 5% of altered glass after 100,000 years (grey curve, Fig. 3b). This study demonstrates that the hypotheses considered in the safety calculations are conservative. Considering a realist scenario based on what is observed and simulated on archaeological glass the quantity of altered glass over the long-term is largely lower.

5. Conclusions

The safety criterion for qualification of a repository is based on the radiation dose received by the populations. In France, for example, the artificial dose added to the natural dose of 2–2.5 mSv/year must not exceed 1 mSv/year (0.25 mSv/year considered in the safety demonstration of the geological disposal [50]). In the case of a nuclear glass or spent fuel repository, this dose is due to a limited number of long-lived, mobile fission products, having a high solubility limit in water and very limited interaction with the host rock (^{129}I, ^{79}Se, ^{135}Cs, ^{36}Cl, etc.) [50]. The dose depends mainly on the properties of the host rock but also on the durability of the containment matrices especially if their lifetimes exceed 50,000 years [50]. In a repository with favorable chemistry (silica-rich medium) and hydraulic properties (low permeability), the long-term behavior models predict that nuclear glasses could immobilize most of the radionuclides during the critical period.

Only the convergence of sound arguments can assess the safety and allow policy makers to reach a decision on the disposition of these materials. This study represents a significant advance toward assessing the uncertainties on nuclear glass alteration rates in the geological repository and improves the confidence in the present mechanistic models. This effort must be pursued with studies on natural analogs altered for longer timescales and in different environments (e.g. in contact with clay minerals) by using the same methodology.

Acknowledgements

We would like to thank C. Fillet, G. Bordier and E. Vernaz for helpful comments. The editor, Lars Werme, and two anonymous reviewers are sincerely acknowledged for their comments which helped us to improve this manuscript. This is CRPG contribution #2077.

References

[1] NEA, Considering Timescales in the Post-closure Safety of Geological Disposal of Radioactive Waste, NEA Report 06426, 2009.
[2] R.C. Ewing, Sci. Basis Nucl. Waste Manage. 1 (1979) 57–58.
[3] R.C. Ewing, Mater. Technol. Adv. Perform. Mater. 16 (2001) 30–36.
[4] J.C. Petit, Appl. Geochem. Suppl. Issue 1 (1992) 9–11.
[5] R.D. Peters, S.C. Slate, Nucl. Eng. Des. 67 (1982) 425–445.
[6] A. Abbas, J.M. Delaye, D. Ghaleb, G. Calas, J. Non-Cryst. Solids 315 (2003) 187–196.
[7] S. Peuget, J.N. Cachia, C. Jégou, X. Deschanels, D. Roudil, V. Broudic, J.M. Delaye, J.M. Bart, J. Nucl. Mater. 354 (2006) 1–13.
[8] E.H. Oelkers, Geochim. Cosmochim. Acta 65 (2001) 3703–3719.
[9] A.F. White, S.L. Brantley, Chem. Geol. 202 (2003) 479–506.
[10] S. Gin, I. Ribet, P. Frugier, T. Chave, F. Angeli, J.E. Lartigue, G. de Combarieu, N. Godon, Assessment of nuclear glass behavior in geological disposal conditions: current state of knowledge and recent advances, in: Eur. Nucl. Conf., Versailles, France, 2005.
[11] K.T.B. MacQuarrie, K.U. Mayer, Earth-Sci. Rev. 72 (2005) 189–227.
[12] S.D. Fontaine, D. Foy, Rev. Arch. Narbonnaise 40 (2007) 235–268.
[13] A. Verney-Carron, S. Gin, G. Libourel, Geochim. Cosmochim. Acta 72 (2008) 5372–5385.
[14] I.C. Freestone, Geomat. Cult. Heritage 257 (2006) 201–216.
[15] B. Berkowitz, P.M. Adler, J. Geophys. Res. 103 (1998) 15339–15360.
[16] J.F. Thovert, P.M. Adler, Geophys. Res. Lett. 31 (2004) 5.
[17] A. Verney-Carron, S. Gin, P. Frugier, G. Libourel, Geochim. Cosmochim. Acta 74 (2010) 2291–2315.
[18] J. van der Lee, L. De Windt, V. Lagneau, P. Goblet, Comput. Geosci. 29 (2003) 265–275.
[19] A. Silvestri, G. Molin, G. Salviulo, J. Non-Cryst. Solids 351 (2005) 1338–1349.
[20] J.M. Perez Jr., J.H. Westsik Jr., Nucl. Chem. Waste Manage. 2 (1981) 165–168.
[21] P. Aagaard, H.C. Helgeson, Am. J. Sci. 282 (1982) 237–285.
[22] A.C. Lasaga, Kinetic Theory in the Earth Sciences, ed. Princeton Series in Geochemistry, 1998.
[23] B. Grambow, R. Müller, J. Nucl. Mater. 298 (2001) 112–124.
[24] B.P. McGrail, A. Kumar, D.E. Day, J. Am. Ceram. Soc. 67 (1984) 463–467.
[25] B.P. McGrail, J.P. Icenhower, D.K. Shuh, P. Liu, J.G. Darab, D.R. Baer, S. Thevuthasen, V. Shutthanandan, M.H. Engelhard, C.H. Booth, P. Nachimuthu, J. Non-Cryst. Solids 296 (2001) 10–26.
[26] G. Geneste, F. Bouyer, S. Gin, J. Non-Cryst. Solids 352 (2006) 3147–3152.
[27] T. Chave, P. Frugier, A. Ayral, S. Gin, J. Nucl. Mater. 362 (2007) 466–473.
[28] I. Friedman, W. Long, Science 191 (1976) 347–352.
[29] A.F. White, H.C. Claasen, Chem. Geol. 28 (1980) 91–109.
[30] N. Tsomaia, S.L. Brantley, J.P. Hamilton, C.G. Pantano, K.T. Mueller, Am. Mineral. 88 (2003) 54–67.
[31] C. Cailleteau, F. Angeli, F. Devreux, S. Gin, J. Jestin, P. Jollivet, O. Spalla, Nat. Mater. 7 (2008) 978–983.
[32] W.H. Casey, Nat. Mater. 7 (2008) 930–932.
[33] P. Frugier, S. Gin, Y. Minet, T. Chave, B. Bonin, N. Godon, J.E. Lartigue, P. Jollivet, A. Ayral, L. De Windt, G. Santarini, J. Nucl. Mater. 380 (2008) 8–21.
[34] F. Delage, J.L. Dussossoy, Mater. Res. Soc. Symp. Proc. 212 (1991) 41–47.
[35] I. Techer, T. Advocat, J. Lancelot, J.M. Liotard, J. Nucl. Mater. 282 (2000) 40–46.
[36] L.J. Criscenti, J.D. Kubicki, S.L. Brantley, J. Phys. Chem. A 110 (2006) 198–206.
[37] T. Advocat, J.L. Crovisier, E. Vernaz, G. Ehret, H. Charpentier, Mater. Res. Soc. Symp. Proc. 212 (1991) 57–64.
[38] C. Guy, J. Schott, Chem. Geol. 78 (1989) 181–204.
[39] P.V. Brady, J.V. Walther, Geochim. Cosmochim. Acta 53 (1989) 2823–2830.
[40] P. Frugier, T. Chave, S. Gin, J.E. Lartigue, J. Nucl. Mater. 392 (2009) 552–567.
[41] J.L. Crovisier, T. Advocat, J.L. Dussossoy, J. Nucl. Mater. 321 (2003) 91–109.
[42] W. Lutze, G. Malow, R.C. Ewing, M.J. Jercinovic, K. Keil, Nature 314 (1985) 252–255.
[43] C.D. Byers, M.J. Jercinovic, R.C. Ewing, K. Keil, Mater. Res. Soc. Symp. Proc. 44 (1985) 583–590.
[44] R.C. Ewing, M.J. Jercinovic, Mater. Res. Soc. Symp. Proc. 84 (1987) 67–86.
[45] R. Cowan, R.C. Ewing, Mater. Res. Soc. Symp. Proc. 127 (1989) 49–56.
[46] M.J. Jercinovic, S.A. Kaser, R.C. Ewing, W. Lutze, Mater. Res. Soc. Symp. Proc. 176 (1990) 355–362.
[47] B. Grambow, Elements 2 (2006) 357–364.
[48] P.K. Abraitis, B.P. McGrail, D.P. Trivedi, F.R. Livens, D.J. Vaughan, Appl. Geochem. 15 (2000) 1399–1416.
[49] E.M. Pierce, E.A. Rodriguez, L.J. Calligan, W.J. Shaw, B.P. McGrail, Appl. Geochem. 23 (2008) 2559–2573.
[50] Andra, Dossier 2005 Argile, Tome Phenomenological Evolution of a Geological Repository, ANDRA Report, C.RP.ADS.04.0025, 2005.
[51] D. Mallants, J. Marivoet, X. Sillen, J. Nucl. Mater. 298 (2001) 125–135.
[52] B. Marty, S. Dewonck, C. France-Lanord, Nature 425 (2003) 55–58.